

## The Crystal Structures of the Rare-Earth Hexaurides $\text{RAu}_6$

BY J. M. MOREAU AND E. PARTHÉ

Laboratoire de Cristallographie aux Rayons X de l'Université, 32 Bd d'Yvoy, CH-1211 Genève 4, Switzerland

(Received 2 March 1974; accepted 14 March 1974)

The crystal structure of  $\text{PrAu}_6$  has been solved by direct methods: monoclinic,  $C2/c$ ,  $a=7.765$  (7),  $b=7.745$  (7),  $c=9.076$  (9) Å,  $\beta=100.3$  (2)°,  $Z=4$ ,  $D_x=16.3$  g cm $^{-3}$ , F.W. 1326.6,  $F(000)=2132$ ,  $R=0.10$ .  $\text{PrAu}_6$  is isotypic with  $\text{CeAu}_6$  and  $\text{NdAu}_6$ . The  $\text{PrAu}_6$  structure type is built up of layers as in  $\beta$ -W, whereas the  $\text{SmAu}_6$  type is constructed of layers as in the  $\sigma$  phase or  $\alpha$ -Mn. Both these structure types can be regarded as built up from an interpenetrating packing of centred polyhedra similar to the Frank-Kasper structures, but in which some of the polyhedra are of a new kind. The Pr and Sm atoms have coordinations 18 and 16 respectively and the Au polyhedra, with coordination 13 or 14, represent a compromise between the icosahedron and the cuboctahedron.

### Introduction

The intermetallic compounds in the lanthanide-gold systems were recently investigated and reviewed by McMasters, Gschneidner, Bruzzone & Palenzona (1971) and Steeb, Gebhardt & Reule (1972). In the 12 R-Au systems (R=La, Ce, Pr, Nd, Sm, Gd, Tb, Dy, Ho, Er, Tm and Lu) these authors reported seven stoichiometries involving 12 structure types and 80 phases. For the stoichiometry  $\text{RAu}_6$  two different undetermined structure types were recognized, one for R=Ce, Pr, Nd and another for R=Sm, Gd, Tb, Dy, Ho. In recent papers (Moreau & Parthé, 1972; Flack,

Moreau & Parthé, 1974) the structure for the medium heavy rare-earth compounds  $\text{RAu}_6$  (R=Sm to Ho) was reported. The present investigation was undertaken in order to resolve the second crystal structure and to elucidate the structural features common to these two new structure types.

### Experimental

The rare-earth metals were obtained from Johnson Matthey and Brandenberger AG (Switzerland) and were 99.9 wt.% pure; the gold obtained from Engelhard Co. (Switzerland) had a purity of 99.999%. The alloys were prepared by conventional arc-melting methods and were then heat-treated in a sealed quartz tube at 700°C for one week. Attempts to isolate single crystals by mechanical means always resulted in plastic deformation. One sample of  $\text{PrAu}_6$  was then ground to a powder which was annealed in a sealed quartz tube at 700°C for three months and from which it was possible to isolate single crystals of about 60  $\mu\text{m}$  diameter.

Lattice constants and intensities were measured with graphite-monochromated Mo  $K\alpha$  radiation and a Philips PW1100 computer-controlled, four-circle goniometer. Intensities could be indexed on the basis of a monoclinic unit cell. The systematic extinction of reflexions with  $h+k$  odd for  $hkl$ , and  $l$  odd for  $h0l$  indicated the space groups  $Cc$  or  $C2/c$ . The lattice parameters of  $\text{PrAu}_6$  obtained by least-squares fit of  $d$  values are  $a=7.765$  (7),  $b=7.745$  (7),  $c=9.076$  (9) Å and  $\beta=100.3$  (2)°. The  $\theta$ - $2\theta$  scan technique was employed to collect all non-equivalent intensities out to a limit of  $(\sin \theta)/\lambda=1$  Å $^{-1}$ . Lorentz and polarization corrections were applied by the method of Levy & Ellison (1960), and absorption corrections were applied with the tabulated values for a spherical crystal (*International Tables for X-ray Crystallography*, 1967) with  $\mu=1771$  cm $^{-1}$ .

All reflexions with intensity less than twice the experimental standard deviation ( $I < 2\sigma$ ) were considered as

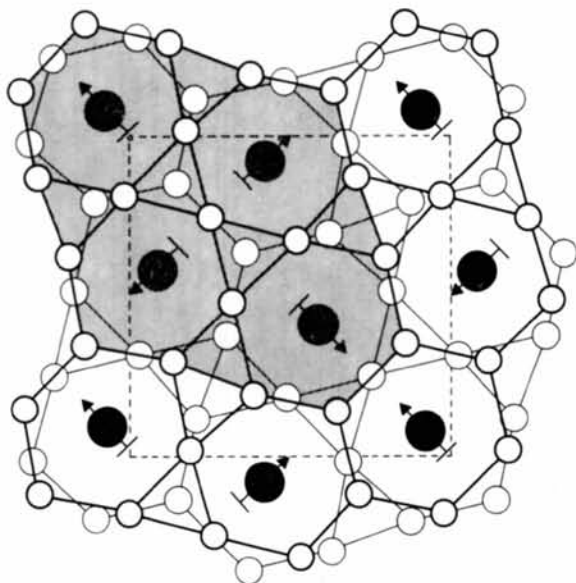


Fig. 1. The arrangement of the hexagonal Au antiprisms centred by Sm atoms in one half ( $0 < z < c/2$ ) of the  $\text{SmAu}_6$  cell. Thick line: upper face; thin line: lower face. The arrows on the Sm atoms indicate the inclination of the antiprisms with respect to the plane of projection. The dashed line indicates the unit cell. A rumpled tile consisting of four antiprisms is shaded. The second secondary layer of Au atoms ( $z=0$  or  $\frac{1}{2}$ ) is not shown.



Table 3. *Interatomic distances in PrAu<sub>6</sub> less than 4 Å*

|              |             |              |             |
|--------------|-------------|--------------|-------------|
| Pr-2Au(2)    | 3.128 (5) Å | Au(2)- Au(1) | 2.738 (5) Å |
| -2Au(2)      | 3.137 (5)   | - Au(3)      | 2.798 (5)   |
| -2Au(1)      | 3.210 (7)   | - Au(3)      | 2.867 (3)   |
| -2Au(2)      | 3.228 (5)   | - Au(3)      | 2.906 (4)   |
| -2Au(3)      | 3.234 (6)   | -2Au(1)      | 2.968 (5)   |
| -2Au(1)      | 3.258 (5)   | - Pr         | 3.128 (5)   |
| -2Au(3)      | 3.289 (4)   | - Pr         | 3.137 (5)   |
| -2Au(3)      | 3.798 (4)   | - Au(2)      | 3.186 (6)   |
| -2Au(1)      | 3.974 (5)   | - Pr         | 3.228 (5)   |
|              |             | - Au(1)      | 3.241 (5)   |
| Au(1)- Au(3) | 2.723 (5)   | - Au(3)      | 3.264 (5)   |
| - Au(2)      | 2.738 (5)   | - Au(2)      | 3.404 (7)   |
| - Au(3)      | 2.763 (7)   |              |             |
| -2Au(1)      | 2.797 (7)   | Au(3)- Au(1) | 2.723 (5)   |
| - Au(3)      | 2.887 (5)   | - Au(3)      | 2.741 (6)   |
| -2Au(2)      | 2.968 (6)   | - Au(1)      | 2.763 (4)   |
| - Pr         | 3.210 (7)   | - Au(2)      | 2.798 (4)   |
| - Au(2)      | 3.241 (5)   | - Au(2)      | 2.867 (4)   |
| - Pr         | 3.258 (5)   | - Au(3)      | 2.882 (6)   |
| - Au(3)      | 3.786 (5)   | - Au(1)      | 2.887 (5)   |
| - Pr         | 3.974 (5)   | - Au(2)      | 2.905 (4)   |
|              |             | - Pr         | 3.234 (6)   |
|              |             | - Au(2)      | 3.264 (5)   |
|              |             | - Pr         | 3.289 (4)   |
|              |             | - Au(1)      | 3.786 (4)   |
|              |             | - Pr         | 3.798 (4)   |

lattice constants of these two compounds together with those of the morphotropic series having the tetragonal SmAu<sub>6</sub> structure type are given in Table 4.

In order to allow recognition of the new structure type a powder pattern calculation [program written by Yvon, Jeitschko & Parthé (1969)] for the low-angle reflexions of PrAu<sub>6</sub> is listed in Table 5. The corresponding calculation for the SmAu<sub>6</sub> structure type can

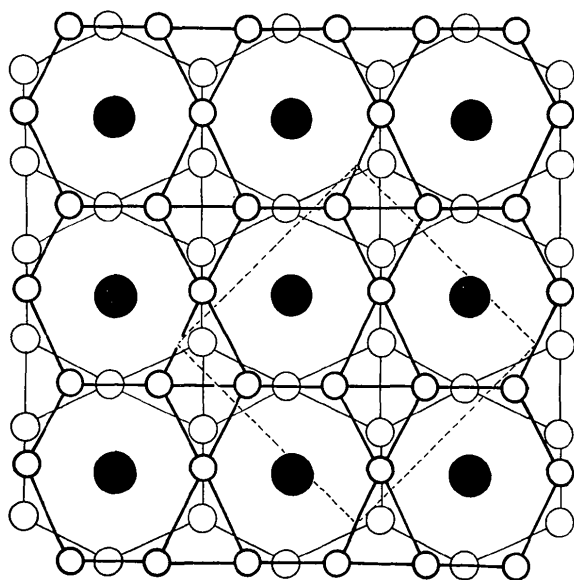


Fig. 2. The arrangement of the hexagonal Au antiprisms centred by Pr atoms in one half ( $0 < z < c/2$ ) of the PrAu<sub>6</sub> unit cell. Thick line: upper face; thin line: lower face. The dashed line indicates the unit cell.

Table 4. *Lattice parameters of RAu<sub>6</sub> compounds*

|                   | <i>a</i> (Å) | <i>b</i> (Å) | <i>c</i> (Å) | $\beta$   | Reference* |
|-------------------|--------------|--------------|--------------|-----------|------------|
| CeAu <sub>6</sub> | 7.80 (1)     | 7.78 (1)     | 9.08 (1)     | 100.6 (3) | (a)        |
| PrAu <sub>6</sub> | 7.765 (7)    | 7.745 (7)    | 9.076 (9)    | 100.3 (2) | (a)        |
| NdAu <sub>6</sub> | 7.74 (1)     | 7.72 (1)     | 9.07 (1)     | 100.1 (3) | (a)        |
| SmAu <sub>6</sub> | 10.395 (6)   | —            | 9.706 (5)    | —         | (b)        |
| GdAu <sub>6</sub> | 10.34 (1)    | —            | 9.71 (1)     | —         | (c)        |
| TbAu <sub>6</sub> | 10.32 (1)    | —            | 9.69 (1)     | —         | (c)        |
| DyAu <sub>6</sub> | 10.30 (1)    | —            | 9.67 (1)     | —         | (c)        |
| HoAu <sub>6</sub> | 10.29 (1)    | —            | 9.66 (1)     | —         | (c)        |

\* (a) This work. (b) Flack, Moreau & Parthé (1974). (c) McMasters, Gschneidner, Bruzzone & Palenzona (1971).

be found in a paper by McMasters & Gschneidner (1973).

Table 5. *Calculated powder data for PrAu<sub>6</sub> for Cr K $\alpha$  radiation ( $\lambda = 2.29092$  Å)*

Intensities calculated from point positions obtained from single-crystal data.  $I = mF^2(1 + \cos^2 2\theta/\sin^2 \theta \cdot \cos \theta)$  is normalized to the strongest line having intensity 1000.

| <i>h</i> | <i>k</i> | <i>l</i> | $\sin^2 \theta \times 10^3$ | Intensity |
|----------|----------|----------|-----------------------------|-----------|
| 1        | 1        | 0        | 44.35                       | 27.7      |
| 1        | 1        | -1       | 53.93                       | 205.1     |
| 0        | 0        | 2        | 65.82                       | 0.0       |
| 1        | 1        | 1        | 67.69                       | 198.7     |
| 0        | 2        | 0        | 87.49                       | 47.7      |
| 2        | 0        | 0        | 89.92                       | 61.0      |
| 1        | 1        | -2       | 96.42                       | 1.2       |
| 0        | 2        | 1        | 103.95                      | 19.2      |
| 1        | 1        | 2        | 123.93                      | 28.9      |
| 2        | 0        | -2       | 128.23                      | 31.5      |
| 0        | 2        | 2        | 153.31                      | 94.2      |
| 1        | 1        | -3       | 171.81                      | 171.3     |
| 2        | 2        | 0        | 177.41                      | 18.0      |
| 2        | 2        | -1       | 180.11                      | 84.5      |
| 2        | 0        | 2        | 183.25                      | 310.8     |
| 2        | 2        | 1        | 207.62                      | 550.8     |
| 1        | 1        | 3        | 213.08                      | 590.7     |
| 2        | 2        | -2       | 215.72                      | 785.1     |
| 1        | 3        | 0        | 219.34                      | 446.6     |
| 3        | 1        | -1       | 220.01                      | 267.2     |
| 3        | 1        | 0        | 224.19                      | 131.8     |
| 1        | 3        | -1       | 228.92                      | 136.0     |
| 0        | 2        | 3        | 235.58                      | 375.4     |
| 1        | 3        | 1        | 242.67                      | 1000.0    |
| 3        | 1        | -2       | 248.74                      | 919.7     |
| 3        | 1        | 1        | 261.28                      | 460.3     |
| 0        | 0        | 4        | 263.27                      | 458.4     |
| 2        | 2        | 2        | 270.74                      | 559.7     |
| 1        | 3        | -2       | 271.40                      | 172.1     |
| 1        | 1        | -4       | 280.11                      | 382.3     |
| 2        | 2        | -3       | 284.24                      | 545.5     |
| 2        | 0        | -4       | 298.17                      | 93.1      |
| 1        | 3        | 2        | 298.91                      | 1.7       |
| 3        | 1        | -3       | 310.38                      | 72.9      |
| 3        | 1        | 2        | 331.27                      | 125.7     |
| 1        | 1        | 4        | 335.13                      | 18.4      |
| 1        | 3        | -3       | 346.80                      | 162.3     |
| 0        | 4        | 0        | 349.97                      | 8.3       |
| 0        | 2        | 4        | 350.76                      | 35.7      |

### Crystal chemistry of hexaaurides

For a description of the PrAu<sub>6</sub> and the SmAu<sub>6</sub> structure types, it is possible to use the concept of primary and

secondary layers as defined by Frank & Kasper (1958).

Primary layers are a tessellation of triangles and hexagons (or pentagons) where the connexions correspond to interatomic distances. Secondary layers consist of triangles and/or squares where the connexions do not correspond to interatomic distances. To characterize the structure in a simple manner, one has to indicate the arrangement of the polygons in these layers. This is conveniently done by means of Schläfli symbols [see, for example, Pearson (1972)].

In  $\text{SmAu}_6$  (Fig. 1) the layers are rumpled but still easily recognizable. There is only one type of primary layer formed by Au atoms, but two types of secondary layers, one consisting of Sm atoms only, the second of Au atoms only. The sequence of the layers is as follows:

|                         |  |                              |
|-------------------------|--|------------------------------|
| Primary layer:          | Au atoms with Kagomé tiling $3636 + 3^26^2 + 6^3(5:4:2)$ | } tile layer shown in Fig. 1 |
| First secondary layer:  | Sm $3^2434$  |                              |
| Primary layer:          | Au $3636 + 3^26^2 + 6^3(5:4:2)$                          |                              |
| Second secondary layer: | Au $4^4$   |                              |

and so on.

The stacking of the first three layers leads to the formation of Sm-centred hexagonal antiprisms. Disregarding for the moment that the layers are not flat, the arrangement of the hexagonal antiprisms is identical with that known for  $\sigma$ -phases. The layers are in fact buckled as in  $\alpha$ -Mn. It is possible to combine four Sm-centred hexagonal antiprisms to form a rumpled tile as shown in Fig. 1. The arrows indicate the inclination relative to the plane of projection. The arrangement of one layer of hexagonal antiprisms may thus be represented by a simple tile pattern where it is sufficient to indicate only the outer contours of the rumpled tiles.

In one unit cell of  $\text{SmAu}_6$  along the  $z$  direction there are eight layers forming two tile layers separated by a secondary layer  $4^4$  of gold atoms.

The  $\alpha$ -Mn and the  $\text{SmAu}_6$  structures – except for the atoms in the second secondary layers – differ in the way the tile layers of hexagonal antiprisms are stacked. Adjacent layers in  $\alpha$ -Mn are displaced by translation, whereas in  $\text{SmAu}_6$  they are rotated by  $90^\circ$ . An explanatory diagram has already been published (Moreau & Parthé, 1972).

Similarly it is possible to describe  $\text{PrAu}_6$  by layers which are only slightly rumpled.

|                  |                         |                |
|------------------|-------------------------|----------------|
| Primary layer:   | Au $3^26^2 + 3636(2:1)$ | } triple layer |
| Secondary layer: | Pr $4^4$                |                |
| Primary layer:   | Au $3^26^2 + 3636(2:1)$ |                |
| Secondary layer: | missing                 |                |

and so on.

It is possible to build up the whole  $\text{PrAu}_6$  structure from two triple layers, one in the normal position and the second upside down and displaced by  $\frac{1}{2}, \frac{1}{4}, 0$  referred to the cubic axes of  $\beta$ -W. An essential difference

with respect to the stacking sequence of  $\text{SmAu}_6$  is the missing second secondary layer of Au atoms between the triple layers. This triple layer can also be interpreted as a planar arrangement of rare-earth centred hexagonal antiprisms as in  $\text{SmAu}_6$  but here connected as in  $\beta$ -tungsten (Fig. 2).

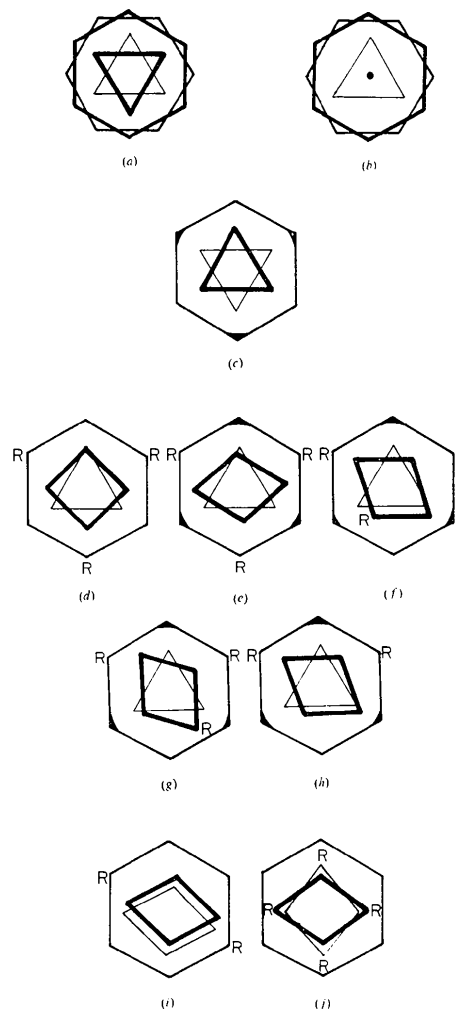


Fig. 3. Schematic drawings of the coordination polyhedra in  $\text{SmAu}_6$  and  $\text{PrAu}_6$ . Thick lines are on top, thin lines on bottom. Thick corners of the hexagon are higher than thin corners. R signifies a rare-earth atom. (a), (b) Coordination around rare-earth atoms: (a) 18 coordination of Pr atoms in  $\text{PrAu}_6$ . Hexagonal antiprism with two triangles, one above and one below. (b) 16 coordination of Sm atoms in  $\text{SmAu}_6$ . Hexagonal antiprism with one triangle below and a single atom on top. (c)–(j) Coordination around gold atoms: (c) 12 coordination. Icosahedron drawn for comparison only. Hexagon in chair configuration with two triangles, one above and one below. (d)–(h) 13 coordination. Top triangle replaced by a square or a rhombus: (d) coordination of Au(2) in  $\text{PrAu}_6$ , (e) coordination of Au(3) in  $\text{SmAu}_6$ , (f) coordination of Au(1) in  $\text{SmAu}_6$ , (g) coordination of Au(1) in  $\text{PrAu}_6$ , Au(3) in  $\text{PrAu}_6$ , (h) coordination of Au(2) in  $\text{SmAu}_6$ . (i) and (j) 14 coordination. Top and bottom triangles replaced by rhombuses: (i) coordination of Au(5) in  $\text{SmAu}_6$ , corresponds to Kasper polyhedron for CN14, (j) coordination of Au(4) in  $\text{SmAu}_6$ .

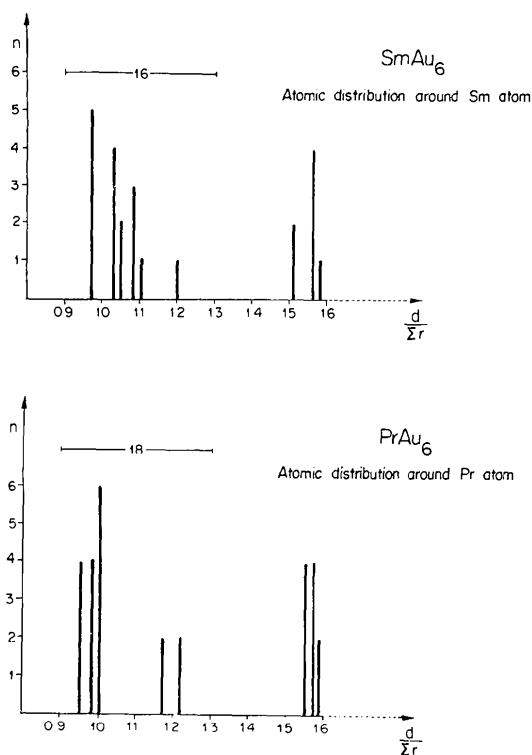


Fig. 4. Atomic distribution around rare-earth atoms in the  $\text{SmAu}_6$  and the  $\text{PrAu}_6$  structure types.  $n$  = number of Au atoms having same distance from rare-earth atom.  $d$  = experimentally determined interatomic distance.  $\sum r$  = sum of rare-earth and Au atom radii for 12 coordination.

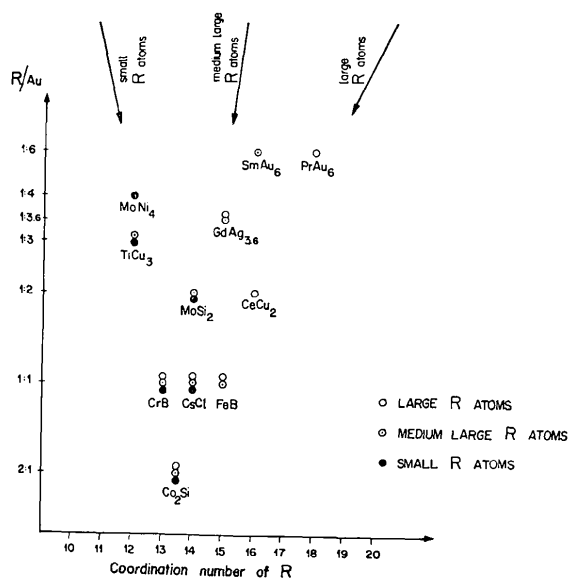


Fig. 5. Lanthanide coordination numbers for the different structure types found with R-Au compounds versus R/Au ratio modified after McMasters, Gschneidner, Bruzzone & Palenzona (1971).

Whereas the description of these structures by layers is certainly useful for an immediate comprehension of the overall geometrical arrangement of the structure, it is the arrangement of the bonding orbitals of the individual atoms and the shape of the individual coordination polyhedra that we are required to explain for a complete understanding of the formation of these structures. The structures can also be described by an interpenetrating packing of polyhedra such that every atom is the *centre* of one polyhedron and at the same time member of the coordination polyhedra of all its neighbours. This is the approach of Kasper (1956).

In Fig. 3, it is possible to distinguish the different types of coordination polyhedra found in  $\text{SmAu}_6$  and  $\text{PrAu}_6$ . The schematic drawings show the connexions between the corners of the polyhedra only when these are parallel or nearly parallel to the plane of projection. As is indicated, one CN 14 polyhedron is similar to the one already described by Frank & Kasper (1958), but all others are of a new kind.

According to the atomic distribution diagram of Fig. 4, Pr has 18, but Sm 16 first gold neighbours. As shown in Fig. 3 the  $\text{PrAu}_{18}$  polyhedron may be characterized as a hexagonal antiprism with a triangle on the top and the bottom. The  $\text{SmAu}_{16}$  polyhedron has also a hexagonal antiprism, a triangle below, but only a single Au atom on top. If the base triangle were rotated by  $30^\circ$  the polyhedron would be the Frank-Kasper polyhedron for CN 16. The gold atoms have 13 or 14 neighbours and have a coordination figure closely related to an icosahedron. As shown in the lower part of Fig. 3, for coordination 13 the upper triangle part has been replaced by a square or a rhombus. With coordination 14 the upper and lower triangles have been replaced by rhombuses. For each group the coordination figures differ only slightly either in the deformation of the square or in the number and arrangement of rare-earth atoms which participate in the coordination figure of the gold atoms. The surface of the Au coordination figures consists of triangles and deformed squares.

There are thus not only tetrahedral but also deformed octahedral interstices in these structures. We find here a compromise between the two space packing principles for metallic structures for which the conditions can be stated as follows.

(1) Atoms of equal size are close packed with equal interatomic distances giving tetrahedra and octahedral interstices.

(2) Atoms of different size are packed with varying interatomic distances such that all interstices are tetrahedral.

An essential difference between the two structure types is seen in the coordination of the rare-earth elements. The size differences of the rare-earth elements due to the lanthanide contraction are responsible for the difference in coordination in these two structure types. The larger, light rare-earth elements can have more Au atoms in the first coordination shell com-

pared with the smaller, heavier rare-earth elements. In general the difference in coordination between the light and the heavy rare-earth elements can be observed only in compounds where the rare-earth element is a minority component such that every rare-earth element is completely surrounded by atoms of another kind.

In Fig. 5, an extension of a diagram given by McMasters, Gschneidner, Bruzzone & Palenzona (1971), the coordination numbers of the rare-earth element for all the different RAu structure types are plotted as a function of the R/Au ratio on a logarithmic scale. Large and small rare-earth compounds of composition R<sub>2</sub>Au have the same structure types and the same coordination.

Only with smaller R/Au ratios does one find different structure types and coordinations for the rare-earth components. The rare-earth coordinations in the two RAu<sub>6</sub> structure types follow the expected trend.

Replacing Au with another element of the same group of the periodic system one finds that RAg<sub>6</sub> compounds do not exist, but CeCu<sub>6</sub> is known (Cromer, Larson & Roof, 1960). Copper is smaller than gold and consequently the coordination polyhedron around Ce has 19 Cu atoms.

We are indebted to Dr H. D. Flack for continuous help and advice in computer programming.

#### References

BUSING, W. R., MARTIN, K. O., LEVY, H. A., BROWN, G. M., JOHNSON, C. K. & THIESSEN, W. E. (1971a). *ORFFE3*. Oak Ridge National Laboratory, Oak Ridge, Tennessee.  
 BUSING, W. R., MARTIN, K. O., LEVY, H. A., ELLISON, R.

D., HAMILTON, W. C., IBERS, J. A., JOHNSON, C. J. & THIESSEN, W. E. (1971b). *ORXFLS3*. Oak Ridge National Laboratory, Oak Ridge, Tennessee.  
 CROMER, D. T., LARSON, A. C. & ROOF, R. B. (1960). *Acta Cryst.* **13**, 913–918.  
 CROMER, D. T. & LIBERMAN, D. (1970). *J. Chem. Phys.* **53**, 1891–1898.  
 FLACK, H. D., MOREAU, J. M. & PARTHÉ, E. (1974). *Acta Cryst.* **B30**, 820–821.  
 FRANK, F. C. & KASPER, J. S. (1958). *Acta Cryst.* **11**, 184–190.  
*International Tables for X-ray Crystallography* (1967). Vol. II. Birmingham: Kynoch Press.  
*International Tables for X-ray Crystallography* (1968) Vol. III. Birmingham: Kynoch Press.  
 KASPER, J. S. (1956). *Theory of Alloy Phases*, pp. 264–276. Cleveland: ASM.  
 LEVY, H. A. & ELLISON, R. D. (1960). *Acta Cryst.* **13**, 270–271.  
 MCMASTERS, O. D. & GSCHNEIDNER, K. A. JR (1973). *J. Less-Common Metals*, **30**, 325–342.  
 MCMASTERS, O. D., GSCHNEIDNER, K. A. JR, BRUZZONE, G. & PALENZONA, A. (1971). *J. Less-Common Metals*, **25**, 135–160.  
 MAIN, P., WOOLFSON, M. M. & GERMAIN, G. (1972). *LSAM, a System of Computer Programs for the Automatic Solution of Centrosymmetric Crystal Structures*. Department of Physics, Univ. of York, York, England.  
 MOREAU, J. M. & PARTHÉ, E. (1972). *C. R. Acad. Sci. Paris*, **274**, 823–826.  
 PEARSON, W. B. (1972). *The Crystal Chemistry and Physics of Metals and Alloys*. Vol. 3. London: John Wiley.  
 STEEB, S., GEBHARDT, E. & REULE, H. (1972). *Mh. Chem.* **103**, 716–735.  
 YVON, K., JEITSCHKO, W. & PARTHÉ, E. (1969). *A Fortran IV Program for the Intensity Calculation of Powder Patterns* (1969 version). Univ. de Genève, Laboratoire de Cristallographie aux Rayons X.

*Acta Cryst.* (1974). **B30**, 1748

## Structural Transformations in Lead Iodide Crystals

BY R. PRASAD AND O. N. SRIVASTAVA

*Department of Physics, Banaras Hindu University, Varanasi 221005, India*

(Received 23 October 1973; accepted 21 February 1974)

Solid-state phase transformations involving basic and long-period lead iodide polytypes have been investigated. The phase transformations have been initiated by annealing the crystals under a vacuum of  $10^{-3}$  to  $10^{-4}$  torr at a temperature of  $260 \pm 20^\circ\text{C}$  for a period of 6 h. While the basic *2H* structure undergoes transformations on each annealing run leading to the creation of new polytypes of higher periodicities, the same is not true for the high-period polytype *12H*. The polytype *12H* does not show any clear-cut change under repeated annealing.

### Introduction

In the past 20 years, much attention has been paid to the phenomenon of polytypism. From an applied point of view, the importance of these studies lies in the preparation of polytypes of known periodicities

which can be used as substitutes for various materials with specific properties (dielectric constant in the case of lead iodide) differing on a known scale. One of the easiest ways to achieve this is through phase transformations where, starting from one polytype, one can develop other polytypes after inducing phase trans-